Rubio-López, A., Artero-Guerrero, J., Pernas-Sánchez, J., & Santiuste, C. (2017). Compression after impact of flax/PLA biodegradable composites. Polymer Testing, 59, 127-135.

doi:https://doi.org/10.1016/j.polymertesting.2017.01.025

Compression after impact of flax/PLA biodegradable composites

A. Rubio-López, J. Artero-Guerrero, J. Pernas-Sánchez, C. Santiuste **

Department of Continuum Mechanic and Structural Analysis, University Carlos III of Madrid, Avda de la Universidad 30, 28911, Leganés, Madrid, Spain

*Corresponding author: Phone +34916249920, csantius@ing.uc3m.es

Abstract.

The study of the impact behaviour and the post-impact residual strength of fully biodegradable composites is presented in this work. To this end, low-velocity impact tests and compressive residual strength tests were carried out on flax/PLA laminates. The results were compared with carbon/epoxy laminates showing some important advantages in terms of absorbed energy and normalized residual strength. The reason was attributed to different energy absorption mechanisms; the main failure mode in flax/PLA laminates is fibre failure while residual strength of carbon/epoxy laminates is dominated by delaminations.

Keywords: A. Fabrics/textiles; B. Impact behaviour; Residual strength

1. INTRODUCTION

With ever increasing awareness of global warming and environmental problems, much attention is being paid to replacing conventional materials with those from renewable sources. Natural fibres as a reinforcing agent is a main focus due to the excellent mechanical properties that it enables [1]. In addition, the use of a biodegradable matrix is worth considering since this would result in a completely biodegradable composite [2,3]. Biocomposites can compete in terms of strength per weight with traditional composites but also in terms of costs [4,5]. One of the main potential applications of biocomposites

is automotive industry due to their energy absorption capability [6]. Vehicle components manufactured with natural fibres can be subjected to crash impacts or stone strikes during its service live. Thus, there is a need to understand the impact and post-impact behaviour of biocomposites laminates.

Energy absorption capability and residual strength are the main variables analysed in impact testing. However, absorbed energy depends on test configuration. Charpy and Izod are the most popular impact tests on biocomposites [7,8]. These tests were originally designed to determinate ductile-brittle transition of materials, therefore they are usually conducted on metals, most often assuming a pre-existing notch, which is not suitable for testing composites. An alternative method is drop-weight test, in which a known mass is dropped from a given height onto a flat, un-notched sample. Drop-weight tests have proven to be valuable source of information about the impact and post-impact behaviour of traditional composites [9-16].

There are some works about low-velocity impact behaviour and residual strength of composites manufactured with natural fibres and non-biodegradable matrices [17-21]. Liang et al. [17] studied flax/epoxy composites, finding delamination combined with transverse cracking, and matrix cracking in the resin-rich zones as the main energy absorption mechanisms during impacts. Residual compressive strength dropped from 30% to 15%, depending on stacking sequence, for specimens impacted at 10J.

Dhakal and his colleagues published several works [18-20] analysing the impact behaviour of hemp/polyester and jute/polyester laminates. They found matrix cracking, delamination and fibre breakage as the predominant failure modes. Post-impact behaviour was studied through flexural after impact (FAI) tests performed on impacted jute/polyester specimens showing a great influence of temperature on residual strength.

Petrucci et al. [21] found a significant reduction of flexural strength, about 90%, when the specimens were impacted at 12J for flax/epoxy laminates and 6J for hemp/epoxy laminates.

However, only one experimental study about low-velocity impact on fully biodegradable composites has been published [22], and post-impact behaviour of biocomposites is an almost unexplored field. Huber et al. [22] developed low-velocity impact on All-Cellulose-Composites (ACC) manufactured from Cordenka fibres. ACC laminates showed a combination of high flexural strength and interfacial adhesion leading to a great energy absorption capability under low-velocity impacts. Rubio-López et al. [23] completed the work of Huber et al. [22] with a numerical analysis of the aforementioned low-velocity impacts on ACC laminates. They developed a numerical model to predict the main failure mechanisms. However, no study about post-impact behaviour of fully biodegradable composites was found.

In an attempt to study the impact behaviour and the after-impact residual strength of fully biodegradable composites, this work presents the analysis of low-velocity impact tests and compressive residual strength of flax/PLA laminates. In order to perform the analysis, a systematic study of the impact has been carried out using the Composite Structure Impact Performance Assessment Program (CSIPAP) proposed by Feraboli and Kedward [28]. The study of the impact behaviour includes the analysis of contact forces, absorbed energy, coefficient of restitution, failure mechanisms, permanent deflections, and damaged area. The influence of hemispherical impactor nose diameter is also analysed. Additionally, results were compared with carbon/epoxy laminates showing that biocomposites present some important advantages in terms of absorbed energy and normalized residual. The following section presents the experimental procedure considering the manufacturing process, the impact methodology and the residual strength

characterization process. In Section 3, the results of these impacts and CAI tests are given. Subsequently a discussion of the results and its relation with the damage mechanisms is proposed. Finally, the conclusions of the work are presented.

2. EXPERIMENTAL PROCEDURE

2.1 Manufacturing

PLA matrix was reinforced with flax woven fibres to manufacture fully biodegradable composites. Flax fibres without chemical pre-treatment were used in a 2x1 basket weave configuration. The matrix was 10361D PLA, a biodegradable thermoplastic resin provided by Natureworks LLC in pellets form. The 10361D PLA is specifically aimed as a binder of natural fibres. The PLA density is 1.24 g/cm^3 and its melting temperature is 145-170ºC.

Composites were manufactured by compression moulding after ply stacking. First, the PLA pellets were placed between two thermoheated plates at a temperature of 185ºC to obtain a uniform film. Then, 5 matrix films were stacked alternatively with the 4 woven plies of 200 mm x 200 mm. The stacked plies were placed between the thermoheated plates. After a 2 minute of pre-heating at 185ºC, 16 MPa pressure was applied during 3 minutes using an universal test machine Servosis ME-404/100. Finally, the biocomposite panels were cooled at room temperature. A thickness of 2.64±0.11 mm resulted after the compression moulding. The quantity of reinforcement was fixed in a weight ratio of 65, as Ochi [24] stated as the optimum value for compression moulding procedures with natural fibres. Composites, fibres and PLA were stored at constant conditions before manufacturing and testing (23ºC, 50% RH). The tensile strength of the resulting biocomposite laminate is 100 MPa. The quality of the manufactured samples was

assessed in a previous work to guarantee the repeatability of the mechanical properties [25], the manufacturing procedure was described in detail in this work.

The manufactured biocomposite panels were cut in square specimens of 80 x 80 mm, they were placed on a steel support and clamped along their outer border in such a way that a circular laminate area of 55 mm in diameter was the effective free span. The specimens were tested at constant conditions of 23ºC and 50% RH.

2.2 Low velocity impact tests

Low-velocity impact tests on manufactured panels were performed by means of an INSTRON-CEAST Fractovis 6875 drop weight tower. The specimens were hit orthogonally with an impactor bar which is free fall accelerated through a guide. At the end of the bar two different diameters of hemispherical nose were placed (12.7 and 20 mm) with different masses of 3.76 kg and 3.815 kg respectively; the impactor bar is instrumented, registering the contact force during the impact. After the impact, an anti-rebound system held the impactor to avoid multi hits on the specimen. Eight impact energies were chosen for each impactor diameter to study the damage threshold energy in the biocomposite laminates and the perforation energy, resulting in 16 test configurations. For each combination of impactor diameter and impact energy two different specimens were impacted, allowing to ensure the repeatability. For each impact configuration, one of the impacted specimens was subjected to Compression After Impact (CAI) tests and the other one was used to analyse the failure modes and the extension of the damage.

2.3 Compression after impact (CAI)

Compression after impact tests were carried out with an Instron 8500 universal testing machine. CAI tests must be carried out in a device that avoids global buckling of the

impacted specimens, so that failure is induced by the damage generated during impact Fig 1c. The CAI device consist in four anti-buckling plates as shown in the scheme of Fig. 1a. The device has a rectangular opening in the middle that left the central surface of the specimen free and did not modify the surfaces damaged by the impact [12]. The dimensions of the set-up were adapted to the geometry of the specimens (80 × 80 mm), Fig. 1b. The two rear plates were welded to the loading plates, the specimens were placed in the set-up and each of the front anti-buckling plates was screwed to the rear plates. A free zone of 4 mm is left between the upper and lower anti-buckling plates.

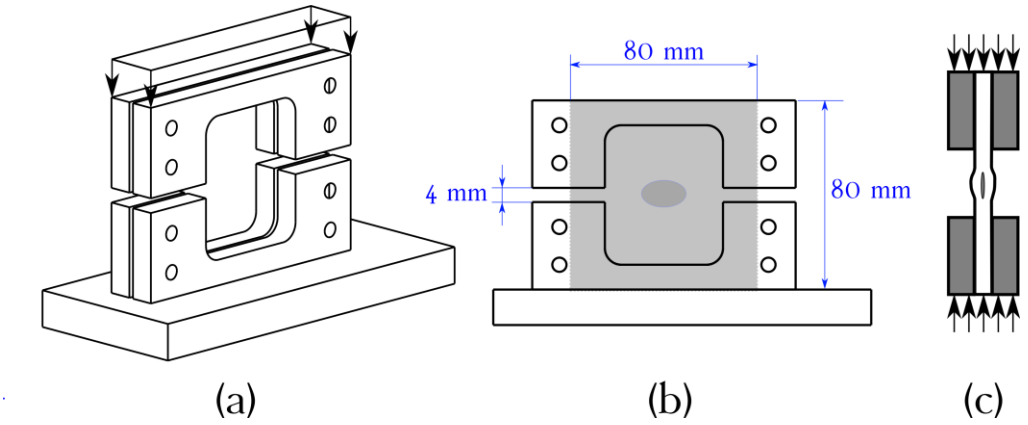

Fig. 1. Compression after impact device. a) Three dimensional sketch. b) front view. c) Failure mode scheme.

2.4 Evaluation and analysis of damage mechanisms

Several techniques were employed to evaluate damage induced by low-velocity impacts: visual inspection, destructive analysis and permanent deflection measurements. Visual inspection was used to identify external damage mechanisms, while destructive analysis was performed to analyse internal damage. The specimens were cut along two perpendicular paths using a diamond saw (Well 3242). Special caution has been taken to avoid any interference in the intra or interlaminar damage for its later analysis, which it has been accomplished using a proper water refrigeration system.

Damage area is usually quantified in traditional composites by ultrasonic inspection because it is determined by delaminations. However, no delaminations were observed in the impacted specimens, thus damaged area was defined using the permanent deflection, similar techniques have been used previously by Wagih et al. [29] relating damaged area with permanent deflection. The damage area was defined by the points with a permanent deflection higher than 1mm. This area was assumed elliptical; thus, two perpendicular axes were measured to calculate damaged area. The permanent deflection in the impacted face was measured by means of a laser extensometer MEL M27L/50. The laser was attached to an automatic positioning system to measure the deflection along a path in the specimen.

3. RESULTS AND DISCUSSION

Impact energy ranged from 3.8 J to 20.0 J. Figs. 2 and 3 show the force-displacement curves obtained with 12.7 mm and 20 mm diameters respectively. Three impact energies were selected to illustrate representative impact tests. The beginning of the curves shows a linear elastic behaviour until the damage onset. The initiation of damage produced a small force drops until peak force is reached; finally contact force drops to zero. The impacts at an energy below the perforation produces a bounce back of the impactor; instead, the laminated impacted at an energy which produces perforation is not able to bounce back the impactor and the displacement increases until contact force drops to zero.

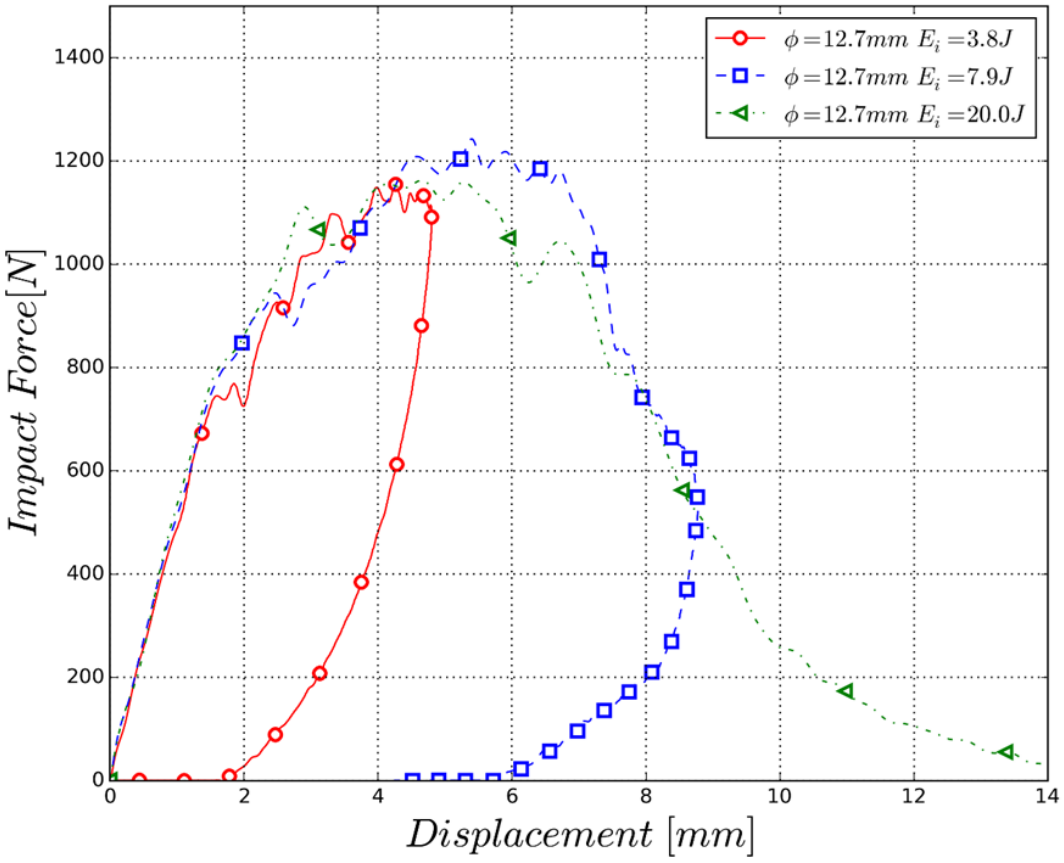

Fig. 2. Force-displacement curves, 12.7 mm diameter impactor. Impact energies = 3.8 J, 7.9 J and 20.0 J.

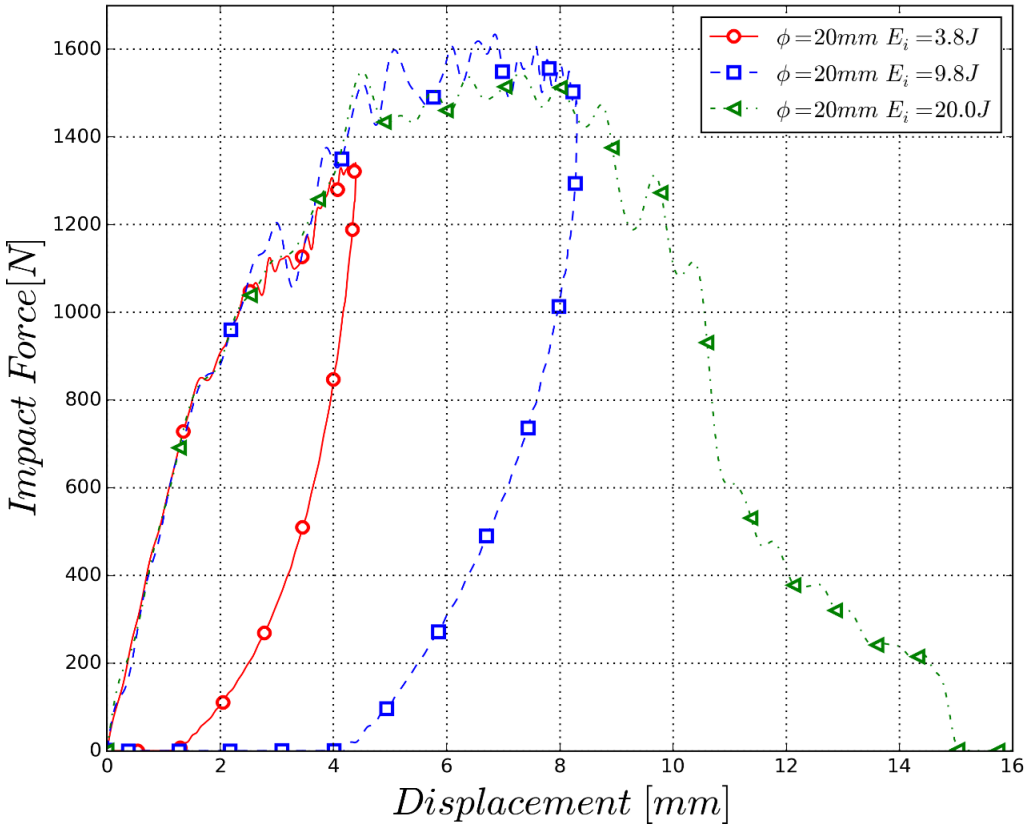

Fig. 3. Force-displacement curves, 20 mm diameter impactor. Impact energies = 3.8 J, 9.8 J and 20.0 J.

The evolution of peak force with impact energy showed two trends, Fig. 4. First, peak force increased with impact energy until 4.7 J using the 12.7 mm nose diameter and 7.9 J with the 20 mm nose diameter. Then, there is a plateau with a peak force of 1200 N and 1600 N for impactor noses of 12.7 mm and 20 mm respectively. The impact energies that divided these two trends corresponded to the onset of a visible crack reducing plate stiffness and, consequently, limiting contact force [30]. Peak forces obtained with 12.7 mm nose diameter were lower than those produced with 20 mm nose diameter due to the stress concentration in the contact area.

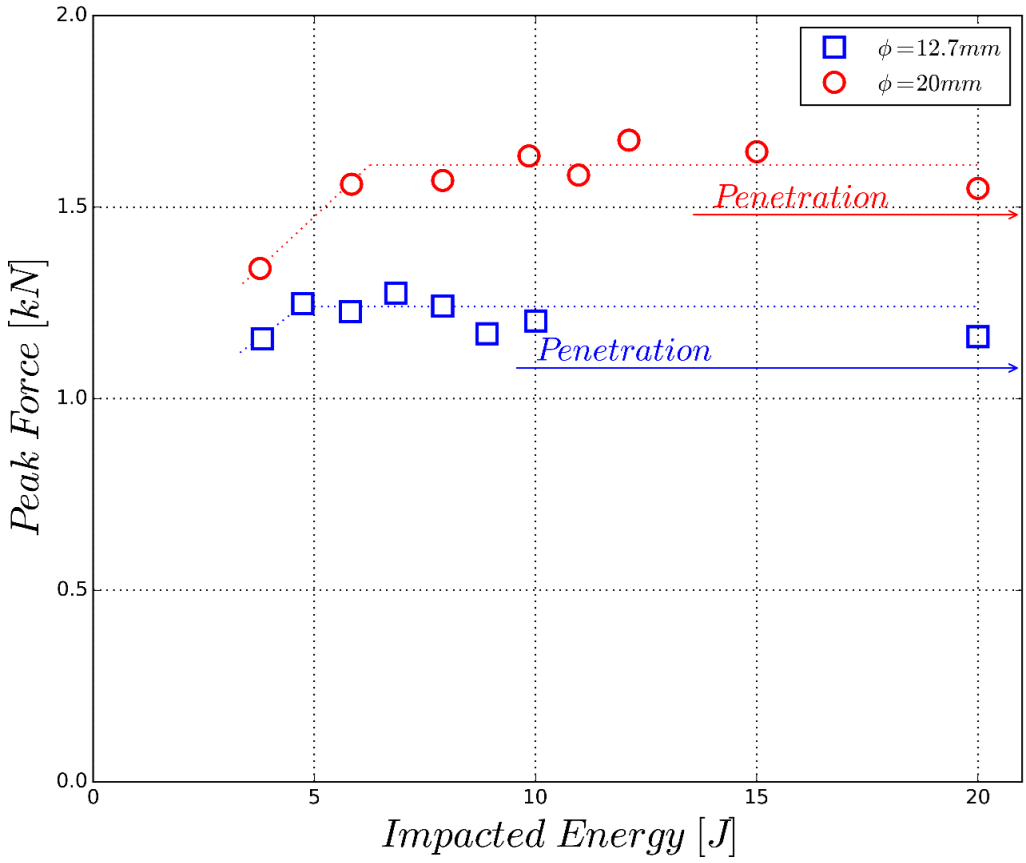

Fig. 4. Peak-force versus impact energy for 12.7 mm and 20 mm nose diameters.

Fig. 5 shows the evolution of absorbed energy with impact energy, two clear stages can be observed. First, there is a linear relationship between impact and absorbed energy. In this first stage, the specimen was damaged but not penetrated by the impactor, thus partial recovery of the energy was produced when the impactor bounced back. The second trend is characterized by the full penetration of the specimen, thus penetration energy was defined as the minimum impact energy that produced the penetration, 10 J and 15 J for the 12.7 mm and 20 mm nose diameters respectively. In the second stage, the maximum energy absorbing capability of the laminate was raised and absorbed energy was stabilized. The smaller impactor nose leaded to a higher stress concentration, thus penetration was produced for lower impact energy.

In addition, Fig. 5 shows the evolution of absorbed energy with impact energy obtained with woven carbon/epoxy laminates [10]. These results were selected because the geometry of plates and impactor was the same that those used in the present work. It should be noticed that flax/PLA laminates absorbed more energy than carbon/epoxy laminates in the same impact conditions. For example, carbon/epoxy plates absorbed 7.1 J when they were impacted at 10 J, while flax/PLA specimens absorbed 7.9 J, meaning an increment of 11.3%. Similar results were found in all the impact energies analysed.

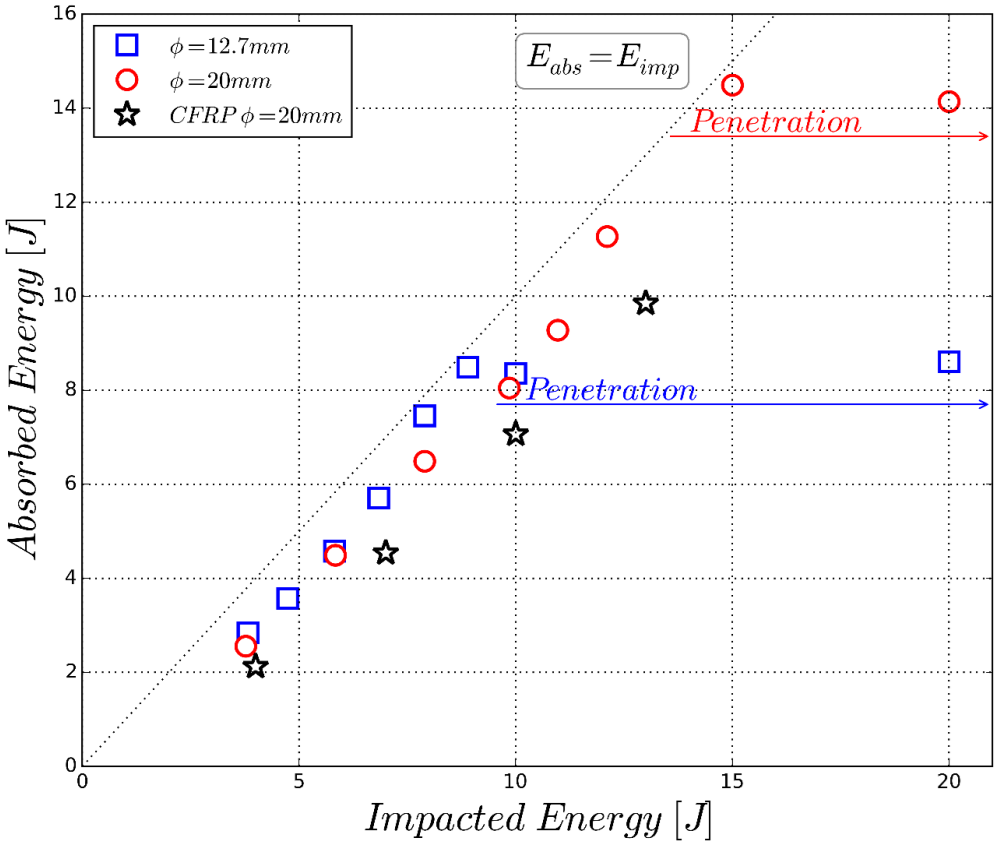

Fig. 5. Absorbed energy versus impact energy for biocomposites using 12.7 mm and 20 mm nose diameters and woven carbon/epoxy composite with the 20 mm nose diameter.

Following the CSIPAP methodology, to study the composite response in terms of energy the coefficient of restitution, COR [11], was calculated as:

$$COR = \sqrt{\frac{E_i - E_a}{E_i}} \quad (1)$$

where E_i is the impact energy and E_a represents the absorbed energy. Upon the penetration, COR decreases as the impact energy increases, due to more energy is dissipated througth failure mechanisms in the composite, Fig. 6. In the case of penetration energy the COR value is zero, all the impact energy is absorbed through the different failure and dissipation mechanisms. The values of penetration energy predicted by COR are in agreement with those showed in Fig. 5. Beyond the penetration, the impact energy is higher than the energy that the laminate is able to absorb/dissipate and the COR increases.

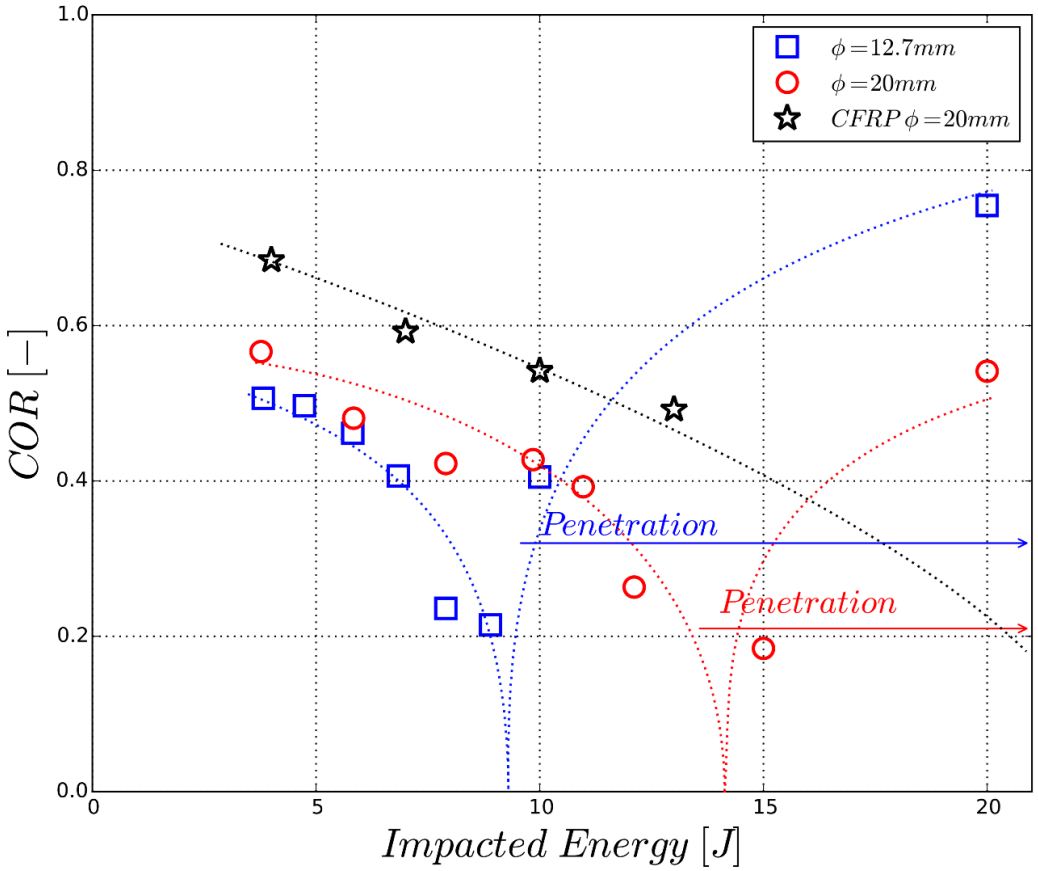

Fig. 6. Coefficient of restitution (COR) vs impact energy.

Normalized residual strength obtained in the CAI test is represented versus the impact energy in Fig. 7. Two trends can be observed; first, a reduction of normalized residual

strength and, second, a plateau for impact energies higher than perforation threshold. The minimum normalized residual strength of perforated laminates is 68% for specimens impacted with the 12.7 mm diameter nose, and 60% for the 20 mm diameter nose, corresponding with the perforation of the specimen. This results are in agreement with the results shown in Fig. 5, the specimens perforated by the bigger impactor nose diameter absorbed more energy and, consequently, their residual strength is lower.

The results of carbon/epoxy woven laminates under the same impact conditions and CAI tests reported by [12] are also included in Fig. 7. It should be noticed that, for the same impact conditions (boundary conditions and impact energy), flax/PLA laminates exhibit a normalized residual strength higher than carbon/epoxy plates. These results can be considered in contradiction with those shown in Fig. 5 because flax/PLA laminates show a higher residual strength even when they absorbed more energy, meaning that they were more damaged. To understand these paradoxical results a detailed analysis of the failure modes and the energy absorption mechanisms in flax/PLA laminates was conducted.

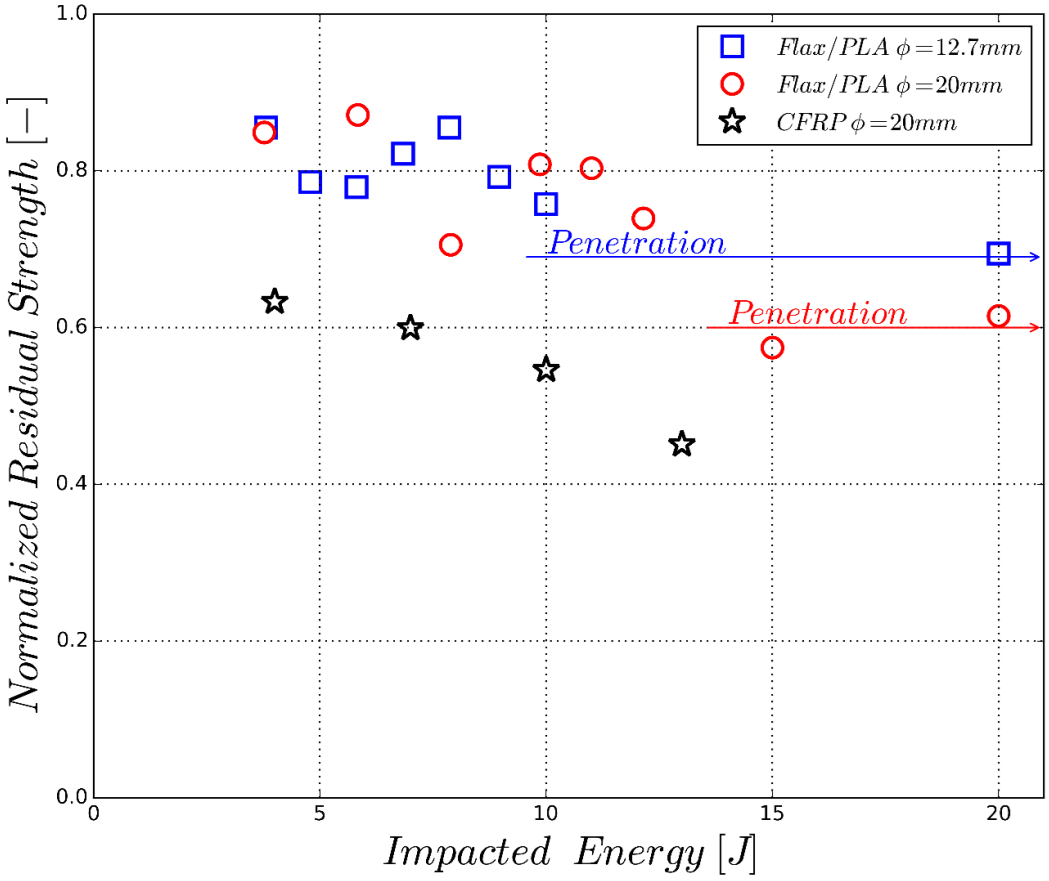

Fig. 7. Normalized residual strength vs impact energy

4. ANALYSIS OF DAMAGE MECHANISMS

Fig. 8 shows front and back faces of specimens impacted by the 12.7 mm impactor at 5.8 J, 7.9 J and 10 J. For the lower impact energy, only fibre failure is observed, it is localized in the back face showing a cross shape typical of woven laminates [11]. The failure appears earlier in the back face because higher strains are produced in this face due to the combined effect of the bending and membrane tensile forces. As impact energy increases, the extension of damage increases in the back face and fibre failure appears also in front face. Finally, in the case of higher impact energy, fibre failure is enough to allow the full penetration of the impactor. It can be seen how the fibre failure in the front face is

rounded, while in the back face has a cross shape creating a pyramidal deformation. This can be explained because in the front face appear a new failure mechanism, the shear failure, while tensile forces are the cause of the failure in the back face. This shear failure occurs only when impact energy is closed to penetration limit or above it. The failure mode with the formation of four petals is similar to that widely reported in studies about impacts on ductile materials as metallic plates. Same conclusions can be obtained in the analysis of the specimens impacted with the 20 mm impactor, in this impact case cracks are larger and the impact energy need to perforate the specimens was higher.

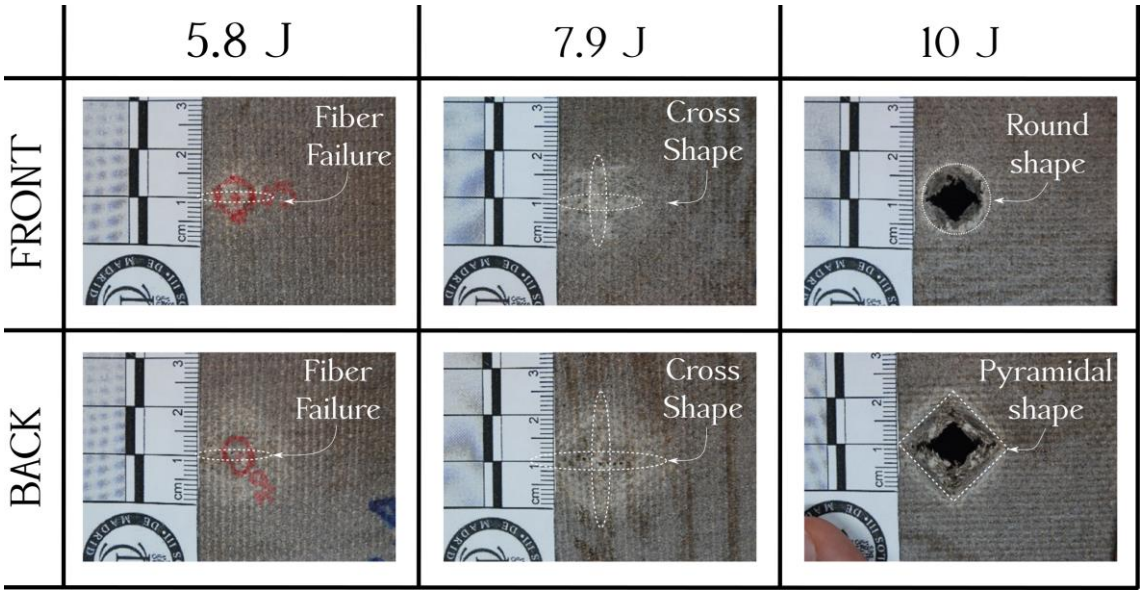

Fig. 8. Photographs of the different failure mechanisms. Impactor nose diameter: 12.7 mm. Impact energies = 5.8 J, 7.9 J and 10 J.

Specimens were cut through its two central paths to analyse internal damage. Pictures of the specimens impacted with the 12.7 mm impactor at 3.8 J, 5.8 J and 10 J are shown in Fig. 9. The main failure mechanism found is fibre failure; matrix cracking was associated with fibre failure while no transverse cracks in resin-rich zones were found; and there

were no delaminations between adjacent plies. Delamination is one of the main failure mechanisms found in traditional composited subjected to low-velocity impacts, thus flax/PLA laminates show a different impact behaviour. The absence of delamination could be explained by the combination of four difference causes: first, delamination produced in woven laminates is smaller than that produced in tape laminates, even in the case of traditional composites [12]; second, the difference between mechanical properties of fibres and matrix is lower than in traditional composites [26]; third, PLA shows a relatively ductile failure in comparison with other matrices as epoxy [27]; finally, the rough surface of natural fibres does not promote the propagation of cracks in the matrix-fibre interface [6]. The first two reasons, woven architecture and lower differences in mechanical properties, could justify minor delaminated areas, but only the last two reasons, ductile failure of PLA and rough surface of natural fibres, can explain the complete absence of delaminations.

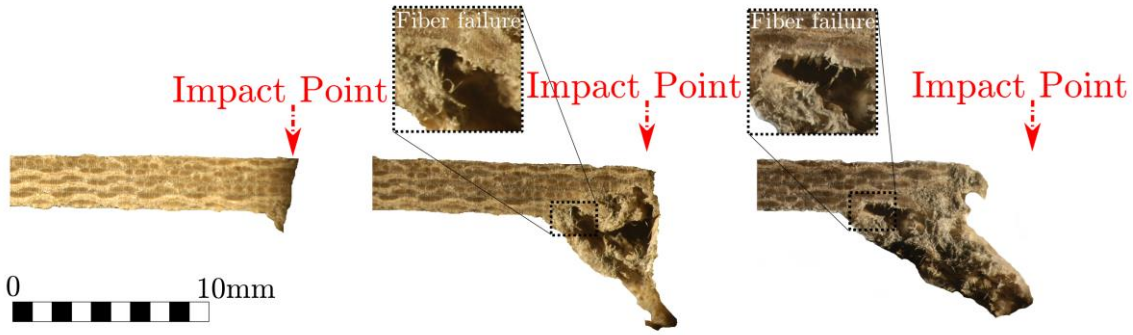

Fig. 9. Photographs of the cut surface. Composites impacted with 12.7 mm impactor. From left to right: 3.8 J, 5.8 J and 10.0 J.

Permanent deflections were measured in all the impacted specimens along two perpendicular paths at the impacted face of the laminate. Fig. 10 shows a path for specimens impacted at different energy levels (3.8 J, 5.8 J, 7.9 J and 10.0 J) with the 12.7

mm diameter impactor. The maximum deflection corresponds to the centre of the plate, while the outer regions (from -40 to -27.5 mm and from 27.5 to 40 mm) were clamped during the test. Both maximum deflection and damaged area increase with impact energy; except in the case of 10.0 J. Damage area decreased when impact energy is higher than penetration energy because damage mechanisms, mainly fibre failure, are in the surrounding of the contact area. Same conclusions can be obtained for the deflections registered in the specimen impacted with the 20 mm impactor.

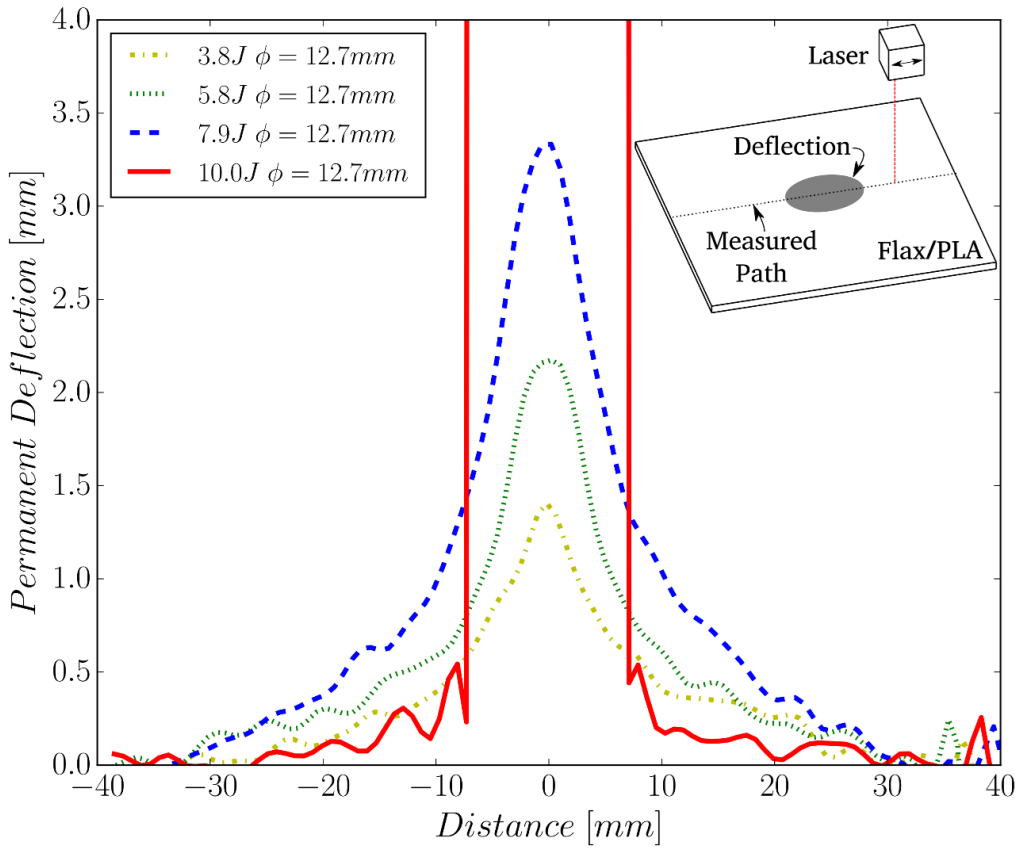

Fig. 10. Permanent deflection vs position for different impact energy. Impactor nose diameter: 12.7 mm.

Following the guidance of studies of low velocity impacts on composites [28, 30], a relationship between the damaged area and residual stiffness has been studied. In traditional composites as carbon/epoxy laminates an increase of damaged area produces

a reduction of residual strength, in order to study if this effect is presented in all biodegradable composites a study of the damage area has been done. First of all, damaged area is represented as function of the impact energy in Fig. 11. Damaged area is defined as the points with permanent deflection higher than 1mm, and it is assumed elliptical, whose axes length were obtained by two perpendicular paths. The evolution of damaged area with impact energy shows three regions. In the first region, damage area increase with impact energy until values near to penetration energy. In the third region, when the specimen was perforated, damaged area is constant with a value slightly higher to the projected surface of the impactor nose. In the transition region, damaged area decreases with impact energy from maximum damage area to the value corresponding to penetration. Therefore, when specimens were perforated the damage was located in the surroundings of the contact area leading to a low reduction in residual strength.

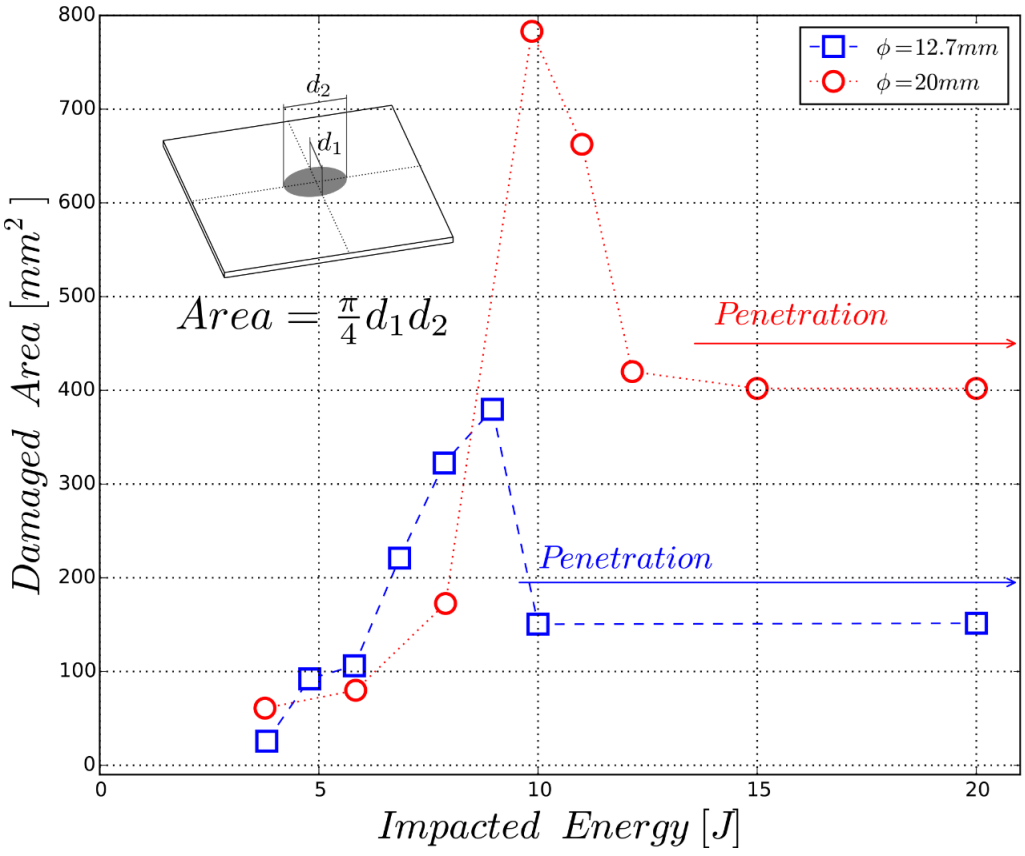

Fig. 11. Damaged area vs impact energy

These different regions observed in the damaged area of the composite laminate cannot be found in the trend of the residual strength presented in Fig. 7; thus, the residual strength is not affected by the damaged area as the traditional composites. The absence of delamination produced that the main contributions to the reduction of residual strength of the laminate is given by the apparition of fibre failure and deflection Fig. 8.

5. CONCLUSIONS

Impact behaviour and residual strength of fully biodegradable composites have been analysed. Two hemispherical impactor noses were compared with diameters of 12.7 mm and 20 mm and impact energy ranged from barely visible damage to penetration. Absorbed energy and COR were used to find the impact energy necessary to produce the full penetration of the laminates, this penetration energy was lower for the 12.7 mm diameter nose. Residual compressive strength was higher in the specimen impacted with the 12.7 mm diameter nose because both, damaged area and absorbed energy, were lower than in specimens impacted with the 20 mm diameter nose.

The present results were compared with tests on carbon/epoxy woven laminates reported in [10] and [12]. These impact and CAI tests were carried out under the same conditions that present work, including specimen geometry. The results showed that fully biodegradable composites as flax/PLA composites present some advantages when they are compared with traditional composites. Flax/PLA woven laminates absorbed more energy under the same impact conditions but their normalized residual strength was higher than that reported in carbon/epoxy plates.

The reasons of this excellent performance of biodegradable composites can be found in the analysis of failure modes. The main failure mode of flax/PLA laminates was fibre failure, while delaminations were not found. This result implies that the energy absorption mechanisms when flax/PLA laminates are subjected to low-velocity impacts are different to those found in traditional composites. Delamination was also found in composites manufactured with natural fibres and non-biodegradable matrices [17-20], thus only the combination of natural fibres and biodegradable matrix can lead to the highest values of normalized residual strength. As a result of the study of the damaged area no relation can be found between this parameter and the residual strength of the impacted laminates.

This is the first study of the after-impact residual strength of fully biodegradable composites; the present results show that this is a promising research field and biocomposites can be suitable for numerous industrial applications. However, more studies must be done to verify these results with other fibres and matrices.

ACKNOWLEDGEMENTS

Authors gratefully acknowledges the support of Spanish Ministry of Economy under the project DPI2013-43994-R.

REFERENCES

[1] U. Wisittanawat, S. Thanawan, T. Amornsakchai. Mechanical properties of highly aligned short pineapple leaf fiber reinforced–nitrile rubber composite: effect of fiber content and bonding agent. Polym. Test,35 (2014), pp20-27.

[2] K. Van de Velde, P. Kiekens. Biopolymers: overview of several properties and consequences on their applications. Polym. Test.21 (2002), pp433-442.

[3] T. Bayerl, M. Geith, A.A. Somashekar, D. Bhattacharyya. Influence of fibre architecture on the biodegradability of FLAX/PLA composites. Int Biodeter Biodegr;96(2014). pp18-25.

[4] A.C. Milanese, M.O.H. Cioffi, H.J.C. Voorwald. Thermal and mechanical behaviour of sisal/phenolic composites. Compos Part B: Eng., 43(2012), pp2843-2850.

[5] A. Porras, A. Maranon. Development and characterization of a laminate composite material from polylactic acid (PLA) and woven bamboo fabric. Compos Part B: Eng. 43(2012), pp2782-2788.

[6] J.D.D. Melo, L.F.M. Carvalho, A.M. Medeiros, C.R.O Souto, C.A. Paskocimas. A biodegradable composite material based on polyhydroxybutyrate (PHB) and carnauba fibers. Compos Part B: Eng. 43(2012), pp2827-2835.

[7] B. Bax. J. Müssig, Impact and tensile properties of PLA/Cordenka and PLA/flax composites, Compos. Sci. Tech. 68(2008), pp1601-1607.

[8] O. Faruk, A.K. Bledzki, H.P. Fink, M. Sain, Biocomposites reinforced with natural fibers: 2000–2010, Prog. Polym. Sci. 37(2012), pp1552–96.

[9] I. Ivañez, C. Santiuste, S. Sanchez-Saez. FEM analysis of dynamic flexural behaviour of composite sandwich beams with foam core. Compos Struct, 92(2010), pp2285-2291.

[10] T. Gómez-del Rio, R. Zaera, E. Barbero, C. Navarro. Damage in CFRPs due to low velocity impact at low temperature. Compos Part B: Eng, 36(2005), pp41-50.

[11] J.A. Artero-Guerrero, J Pernas-Sánchez, J. López-Puente, D. Varas. Experimental study of the impactor mass effect on the low velocity impact of carbon/epoxy woven laminates. Compos Struct, 133(2015), pp774-781.

[12] S. Sánchez-Sáez, E. Barbero, R. Zaera, C. Navarro. Compression after impact of thin composite laminates.Compos Sci Tech; 65(2005), pp1911-1919.

[13] C. Santiuste, S. Sánchez-Sáez, E. Barbero. A comparison of progressive-failure criteria in the prediction of the dynamic bending failure of composite laminated beams.Compos Struct, 92(2010), 2406-2414.

[14] C. Santiuste, S. Sánchez-Sáez, E. Barbero. Residual flexural strength after low-velocity impact in glass/polyester composite beams. Compos Struct, 92(2010):25-30.

[15] I.M. De Rosa, F. Sarasini. Use of PVDF as acoustic emission sensor for in situ monitoring of mechanical behaviour of glass/epoxy laminates, Polym. Test. 29 (2010), pp749–758.

[16] H. Daiyan, E. Andreassen, F. Grytten, O.V. Lyngstad, T. Luksepp, H. Osnes. Low velocity impact response of injection-moulded polypropylene plates-part 1: effects of plate thickness, impact velocity and temperature, Polym. Test. 29 (2010), pp648–657.

[17] S. Liang, L. Guillaumat, P.B. Gning. Impact behaviour of flax/epoxy composite plates. Int J Impact Eng, 80(2015), pp56-64.

[18] H.N. Dhakal, Z.Y. Zhang, M.O.W. Richardson, O.A.Z. Errajhi. The low velocity impact response of non-woven hemp fibre reinforced unsaturated polyester composites. Compos Struct, 81(2007), pp559-567.

[19] H.N. Dhakal, V. Arumugam, A. Aswinraj, C. Santulli, Z.Y. Zhang, A. Lopez-Arraiza. Influence of temperature and impact velocity on the impact response of jute/UP composites. Polym. Test. 35(2014), pp10-19.

[20] H.N. Dhakal, Z.Y. Zhang, N. Bennett, P.N.B. Reis. Low-velocity impact response of non-woven hemp fibre reinforced unsaturated polyester composites:

Influence of impactor geometry and impact velocity. Compos Struct, 94(2012), pp2756-2763.

[21] R. Petrucci, C. Santulli, D. Puglia, E. Nisini, F. Sarasini, J. Tirillò, J.M. Kenny. Impact and post-impact damage characterisation of hybrid composite laminates based on basalt fibres in combination with flax, hemp and glass fibres manufactured by vacuum infusion. Compos Part B: Eng, 69(2015), pp507-515.

[22] T. Huber, S. Bickerton, J. Müssig, S. Pang, M.P. Staiger. Flexural and impact properties of all-cellulose composite laminates. Compos Sci Tech, 88(2013), pp92-98.

[23] A. Rubio-López, A. Olmedo, C. Santiuste. Modelling impact behaviour of all-cellulose composite plates. Compos Struct, 122(2015), pp139-143.

[24] S. Ochi. Mechanical properties of kenaf fibers and kenaf/PLA composites. Mech mater, 40(2008), pp446-52.

[25] A. Rubio-Lopez, A. Olmedo, A. Diaz-Alvarez, C. Santiuste. Manufacture of compression moulded PLA based biocomposites: A parametric study. Compos Struct, 131(2015), pp995-1000.

[26] G. Koronis, A. Silva, M. Fontul. Green composites: a review of adequate materials for automotive applications. Compos Part B: Eng, 44(2013), pp120-127.

[27] N. Graupner, A.S. Herrmann, J. Müssig. Natural and man-made cellulose fibre-reinforced poly (lactic acid)(PLA) composites: An overview about mechanical characteristics and application areas. Compos Part A, 40(2009), pp810-821.

[28] Feraboli P, Kedward KT. A new composite structure impact performance assessment program. Compos Sci Technol 2006;66:1336–47.

[29] A. Wagih, P. Maimí, E.V. González, N. Blancom J.R. Sainz de Aja, F.M. de la Escalera, R. Olsson, E. Alvarez. Damage sequence in thin-ply composite

laminates under out-of-plane loading . Composites Part A: Applied Science and Manufacturing 87, pp 66 - 77, 2016

[30] J.A. Artero-Guerrero, J. Pernas-Sánchez, J. López-Puente, D. Varas, Experimental study of the impactor mass effect on the low velocity impact of carbon/epoxy woven laminates, Composite Structures, Volume 133, 1 December 2015, pp774-781

Figure captions

Fig. 1. Compression after impact device. a) Three dimensional sketch. b) front view. c) Failure mode scheme.

Fig. 2. Force-displacement curves, 12.7 mm diameter impactor. Impact energies = 3.8 J, 7.9 J and 20.0 J.

Fig. 3. Force-displacement curves, 20 mm diameter impactor. Impact energies = 3.8 J, 9.8 J and 20.0 J.

Fig. 4. Peak-force versus impact energy for 12.7 mm and 20 mm nose diameters.

Fig. 5. Absorbed energy versus impact energy for biocomposites using 12.7 mm and 20 mm nose diameters and woven carbon/epoxy composite with the 20 mm nose diameter.

Fig. 6. Coefficient of restitution (COR) vs impact energy.

Fig. 7. Normalized residual strength vs impact energy

Fig. 8. Photographs of the different failure mechanisms. Impactor nose diameter: 12.7 mm. Impact energies = 5.8 J, 7.9 J and 10 J.

Fig. 9. Photograph of the cut surface. Composites impacted with 12.7 mm impactor. From left to right: 3.8 J, 5.8 J and 10.0 J.

Fig. 10. Permanent deflection vs position for different impact energy. Impactor nose diameter: 12.7 mm.

Fig. 11. Damaged area vs impact energy